encit 2020

ABCM Associação Brasileira de Engenharia e Ciências Mecânicas

18th Brazilian Congress of Thermal Sciences and Engineering
November 16-20, 2020 (Online)

ENC-2020-0399
ANALYSIS OF ERROR PROPAGATION IN THE MEASUREMENT OF LAMINAR FLAME SPEED USING CONSTANT VOLUME REACTOR

João Paulo Furlanetto Miranda
Jônatas Vicente
Amir Antônio Martins de Oliveira Jr.
Department of Mechanical Engineering, Federal University of Santa Catarina, Campus João David Ferreira Lima, Bairro Trindade, Florianópolis, SC, Brazil.
joao.miranda@labcet.ufsc.br, jonatas.vicente@labcet.ufsc.br, amir.oliveira@gmail.com

Abstract. *The present study aims at estimating the uncertainties in the measurement of laminar flame speed in a constant volume reactor (CVR). In this laboratory equipment, the laminar flame speed of air-fuel mixtures is measured indirectly from the optical observation of the outwardly propagation of a spherical flame. The measurement random errors in the values of laminar flame speed originate from random errors in the mass filing of the reactor with fuel and air, in the initial pressure and temperature of the reacting mixture, in the acquisition and treatment of the high-speed visible images and on the mathematical treatment of the effects of flame stretch. The random errors in these variables propagate in a complex way to compose the final measurement error. In this work, a Monte Carlo technique is used to assess the error propagation. The calculations were performed in Matlab. For the common conditions found in the measurement of laminar flame speed for liquid hydrocarbon fuels, the propagation of random errors resulted in uncertainties that range from* $\pm$ *3.5 % at stoichiometric ratios of 0.7 and 1.4, to* $\pm$ *0.8 % around the stoichiometric ratio of 1.1, where the effects of random errors reduce to a minimum. The errors in unburned temperature have the greatest importance for fuel lean mixtures and those in unburned pressure and mass of fuel are the most important for fuel rich mixtures. Higher temperatures reduce the effect of temperature in the overall errors.*

Keywords: *Laminar flame speed. Constant volume reactor. Error propagation. Monte Carlo method.*

1. INTRODUCTION

The laminar flame speed is an important physical-chemical characteristic of the fuel-oxidant mixtures. It affects heat release, flammability limits, flame stability and emissions (Law, 2010). There are several methods to measure the laminar flame speed (Egolfopoulos, 2012). The constant volume reactor (CVR) confines the premixed reactant mixture in a closed vessel, usually cylindrical or spherical, promotes a central spark ignition and follows the outwardly propagation of the laminar flame front (Bonhomme *et al.*, 2013; Omari and Tartakovsky, 2016; Park *et al.*, 2016; Lefebvre *et al.*, 2016; Xiouris *et al.*, 2016; Giannakopoulos *et al.*, 2019; Faghih *et al.*, 2019; Bradley *et al.*, 2019). The position of the flame surface is measured along time from the ignition. From the treatment of the image data, the laminar flame speed in indirectly determined (Kelley and Law, 2009; Chen, 2011; Lipatnikov *et al.*, 2015; Wu *et al.*, 2015; Liang *et al.*, 2017; Huo *et al.*, 2018; Beeckmann *et al.*, 2019). The method has the intrinsic disadvantage of producing stretched laminar flames subjected to unburned pressure and temperature variations, heat loss and instabilities (Jayachandran *et al.*, 2014; Yu *et al.*, 2014; Bauwens *et al.*, 2019). Conversely, the method has the advantages of using small amounts of fuel, allowing for fast measurements and for the measurement of flame speeds in high unburned temperatures and pressures, typical of the applications in internal combustion engines (Moghaddas *et al.*, 2012). Therefore, it has been used extensively since the 1960's. Recently, the errors induced by the mathematical treatment of the image measurements have been addressed both experimentally and by simulation and several guidelines have been suggested (Chen, 2015; Jayachandran *et al.*, 2015; Xiouris *et al.*, 2016). However, there is still a need to quantify the effects of the random errors in the measurement of the input variables, i.e., temperature, pressure and mass, in the output results, i.e., equivalence ratio and laminar flame speed. This quantification allows for correctly expressing the uncertainties in the reported results and also for improvements in the experimental set-up.

In the CVR method, each measurement starts with the evacuation, heating and feeding of the reactor. The evacuation aims at removing all traces of previous experiments and creating a low pressure condition that favors the liquid fuel vaporization. The heating of the reactor sets the unburned mixture temperature T_u (K). Then, according to the equivalence ratio Φ (nond.) desired, a given mass of fuel m_f (g) is injected and flash vaporized. Then, dry air is injected until the total pressure reaches the unburned mixture pressure p_u (kPa) desired. The reactor is let to reach thermal equilibrium at

T_u and all flow caused by the air injection is dissipated by viscous dissipation, producing a stagnant mixture. Now, the ignition is done, image acquisition occurs and the analysis follows. During the first stages of flame propagation the reactor pressure deviates less than 10 % of the initial unburned pressure and this is called the constant pressure period. When the pressure reaches about 1.1 times the initial pressure, the flame front has displaced about 30 % of the reactor volume. The confinement of the reactor walls cause the pressure to increase at increasingly higher rates until reaching the maximum pressure, controlled by the amount of energy contained in the unburned mixture, the composition, the reactor volume and the heat loss to the reactor walls. The image analysis is performed in the constant pressure regime and, therefore, the pressure may be assumed constant during flame propagation. For a given fuel-air mixture, usually a minimum of 3 measurements are performed. Periodically, the reactor is open and cleaned, with special care of the windows and seals. Therefore, a thorough measurement of the laminar flame speed for a fuel at different equivalence ratios, unburned temperature and pressure is a time-consuming effort (Monteiro, 2015).

To improve the accuracy of the measurements and reduce the number of experiments needed for a given characterization, the uncertainties in stoichiometric ratio, unburned temperature and pressure, and the consequent propagation of these errors to the laminar flame speed, must be minimized. A starting point is to known the importance of each of these errors in compounding the final measurement uncertainty in the laminar flame speed.

Here, we use the Monte Carlo technique (Herrador and Gonález, 2004) to produce a large sample of virtual measurements affected by random errors in the input variables and evaluate the statistical properties of the large ensemble of final values of laminar flame speed. In the following, we first review the basis of the measurement method, we then describe the application of the Monte Carlo technique, present and analyze the results, and finally draw a few conclusions about error minimization in the application of the CVR method.

2. MEASUREMENT PRINCIPLE AND EQUIPMENT

2.1 Outwardly propagating laminar premixed flame

Figure 1 presents a sector of a Schlieren photograph of a spherical, outwardly propagating, laminar, premixed flame (Adapted from Monteiro (2015)). The ignitors are located in the center of the reactor and at this time instant the flame surface has a radius R_F. The burned mixture occupies the region within the flame surface, at $r < R_F$, and the unburned mixture lays outside the flame surface, at $r > R_F$. In this figure, the velocities of the unburned and burned mixtures are u_u and u_b, and the unburned and burned flame speeds are S_u and S_b, respectively. All velocities are assumed normal to the flame surface.

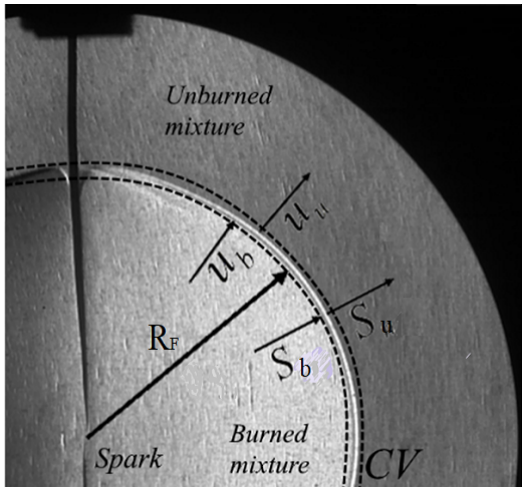

Figure 1. Schlieren photograph of a propagating flame, depicting the flame radius R_F, the speeds of the unburned and burned mixtures u_u and u_b normal to the flame sheet, and the unburned and burned flame speeds S_u and S_b, respectively. (Adapted from Monteiro (2015)).

In a plane, stationary, laminar premixed flame, the *laminar flame speed* S_L is equal to the *flame consumption speed*, i.e., the speed in which the reactant mixture is consumed in the flame. It is also equal to the *flame displacement speed*, i.e., the speed in which the unburned fuel mixture moves towards the flame. This is not true for the outwardly expanding (transient) flame.

For the transient, outwardly expanding flame, the speed of the moving flame front measured in respect to a coordinate system fixed in the center of the spherical reactor, named *flame displacement speed* S_F, is determined from the time

recording of the flame position R_F as

$$S_F = \frac{dR_F}{dt}. \tag{1}$$

An overall mass conservation over a control volume around the flame sheet (see Fig. 1) moving with speed S_F provides

$$R_u^2 \rho_u \left(u_u - S_F\right) = R_b^2 \rho_b \left(u_b - S_F\right), \tag{2}$$

or,

$$R_u^2 \rho_u S_u = R_b^2 \rho_b S_b, \tag{3}$$

where ρ_u and ρ_b are the density of the unburned and burned mixtures, and $u_u = \left[(\mathbf{u}\cdot\mathbf{n})\right]_u$ and $u_b = \left[(\mathbf{u}\cdot\mathbf{n})\right]_b$ are the speeds of the unburned and burned mixtures in respect to the coordinate system fixed in the center of the spherical reactor at positions R_u and R_b.

This kinematic description carries a number of ambiguities already noted before (Bonhomme *et al.*, 2013). First, the flame position R_F is an artifact of the flame surface detection technique, usually, a shadow or schlieren flame visualization technique. Secondly, the flame surface is not sharp, but has a flame thickness of the order of $\ell_T \sim \alpha/S_u$, where α is the thermal diffusivity (the reaction zone has a characteristic length scale of the order of $\beta^{-1}\ell_T$ where β is the Zeldovich number). Therefore, the overall mass balance carries an ambiguity related to where the position of the flame surface, R_F, is defined and where the variables ρ_u, ρ_b, u_u and u_b are measured. Moreover, the unburned mixture speed u_u is formed by two components. One component is the *flame conversion speed* S_u, i.e., the speed in which the unburned mixture crosses the flame front as reactants are converted to products. The second component derives from the outward movement of the unburned mixture towards the reactor wall as a result of the expansion of the burned mixture downstream from the flame front. Since the flame is initiated in the center of the reactor, the burned mixture is progressively compressed towards the center of the reactor as the flame moves outwardly. This results in an inward burned mixture speed u_b. This complex interplay of fluid motion renders it difficult to unambiguously define the conversion speed S_u for the outwardly expanding flame from kinematic arguments only.

Bonhomme *et al.* (2013) proposed a mass balance approach. The equation for the conservation of the mass of chemical species i, assuming spherical symmetry, is given as

$$\frac{\partial}{\partial t}\left(\rho Y_i\right) + \frac{1}{r^2}\frac{\partial}{\partial r}\left[r_2 \rho Y_i \left(u + V_i\right)\right] = M_i \dot{w}_i, \tag{4}$$

where Y_i is the mass fraction of species i, u is the mass averaged flow speed, V_i is the diffusion velocity of species i and $\dot{w}_i$ is the molar production rate of species i.

Integrating from $r = 0$ to $r = R_o$, where R_o is the radius of the spherical reactor, we obtain

$$\frac{dm_i}{dt} + \left[4\pi r^2 \rho Y_i \left(u + V_i\right)\right]_{r=R_o} = 4\pi M_i \int_0^{R_o} \dot{w}_i r^2 dr, \tag{5}$$

where,

$$m_i = 4\pi \int_0^{R_o} \rho Y_i r^2 dr, \tag{6}$$

is the total mass of species i contained in the reactor.

Using Eq. (3) for the consumption speed S_u, the conservation of mass of species i becomes

$$\frac{dm_i}{dt} + \left[4\pi r^2 \rho Y_i \left(u + V_i\right)\right]_{r=R_o} = 4\pi R_u^2 \rho_u S_u (Y_{i,u} - Y_{i,b}). \tag{7}$$

Let us take species i as a product species, say $\mathrm{CO_2}$, $Y_{\mathrm{CO_2}}(r = R_o) = 0$. Then,

$$m_{\mathrm{CO_2}} = 4\pi \int_0^{R_o} \rho Y_{\mathrm{CO_2}} r^2 dr. \tag{8}$$

Assuming that the mass concentration of $\mathrm{CO_2}$, $\rho_b Y_{\mathrm{CO_2},b}$, is uniform within the burned mixture and zero in the unburned mixture region, we have

$$m_{\mathrm{CO_2}} = \frac{4\pi}{3} R_F^3 \rho_b Y_{\mathrm{CO_2},b}. \tag{9}$$

We notice that, in fact, R_F becomes defined by Eq. (9), i.e., R_F is the radius of the sphere that encompasses the entire mass of CO_2 at any given instant of time. Then, writing the conservation of mass of CO_2 we have

$$\frac{dm_{\mathrm{CO}_2}}{dt} = -4\pi R_o^2 \rho_u S_u Y_{\mathrm{CO}_2,b}, \tag{10}$$

and replacing m_{CO_2} by Eq. (9), we obtain

$$\frac{dm_{\mathrm{CO}_2}}{dt} = \frac{d}{dt}\left[\frac{4}{3}\pi R_F^3 \rho_b Y_{\mathrm{CO}_2,b}\right] = 4\pi R_F^2 \rho_b Y_{\mathrm{CO}_2,b}\frac{dR_F}{dt} = -4\pi R_u^2 \rho_u S_u Y_{\mathrm{CO}_2,b}, \tag{11}$$

or,

$$S_u = \frac{\rho_b}{\rho_u}\frac{R_F^2}{R_u^2}\frac{dR_F}{dt}. \tag{12}$$

Now we can make a final flame sheet assumption by defining $R_u = R_F$. Therefore,

$$S_u = \frac{\rho_b}{\rho_u}\frac{dR_F}{dt}. \tag{13}$$

In summary, the hypothesis defining the flame speed are:

1. The experimentally detected flame position R_F is the radius of the sphere that encompasses the entire mass of CO_2 at any given instant of time.
2. The mass concentration of CO_2, $\rho_b Y_{\mathrm{CO}_2,b}$, is uniform within the burned mixture and zero in the unburned mixture region.
3. The position where the conversion velocity S_u is defined is the same as the experimentally detected flame position, $R_u = R_F$.

The speed of the outwardly propagating spherical flame is affected by flame stretch. The flame stretch rate $\mathcal{K}$ is defined as

$$\mathcal{K} = \frac{1}{A_F}\frac{dA_F}{dt}, \tag{14}$$

where A_F is the flame surface area. The flame stretch rate is a measure of the deformation of the flame surface resulting from its motion and the underlying hydrodynamic strain. For the outwardly propagating spherical flame, $A_F = 4\pi R_F^2$ and

$$\mathcal{K} = \frac{2}{R_F}\frac{dR_F}{dt}. \tag{15}$$

Thus, the outwardly propagating spherical flame is positively stretched, i.e., it is extended.

For stretched flames, the laminar flame speed S_L has been related to the consumption speed S_u as

$$S_u = S_L - \mathcal{L}\,\mathcal{K}, \tag{16}$$

where $\mathcal{L}$ is the Markstein length. This equation is known as the *linear model*.

In a more comprehensive model(Kelley and Law, 2009), the laminar flame speed S_L has been related to the consumption speed S_u as

$$\left(\frac{S_u}{S_L}\right)^2 \ln\left(\frac{S_u}{S_L}\right)^2 = -\frac{2\mathcal{L}}{S_L}\mathcal{K}, \tag{17}$$

where, as above, $\mathcal{L}$ is the Markstein length. This equation is known as the *non-linear model*.

In summary, the method of measuring the laminar flame speed in a CVR consists in:

1. Measuring the R_F as a function of time t while the pressure increase remains below 10 % of the initial pressure p_u.
2. Extracting the time derivative of R_F, $\dot{R}_F = dR_F/dt$, using some smoothing technique.
3. Calculating the stretch rate $\mathcal{K} = 2\dot{R}_F/R_F$.
4. Calculating the flame speed in respect to the unburned mixture $S_u = \dot{R}_F/E$, where $E = \rho_u/\rho_b$ is the expansion ratio.
5. Curve fitting the linear model, Eq. (16), obtaining first estimates of S_L and $\mathcal{L}$.
6. Curve fitting the non-linear model, Eq. (17), obtaining the final estimates of S_L and $\mathcal{L}$.
7. Evaluating the statistical uncertainties in S_L and $\mathcal{L}$.

2.2 Experiment and data treatment

Figure 2 presents the experimental apparatus developed by (Hartmann, 2014; Monteiro, 2015). The CVR consists of two stainless-steel hemispheres that form an 150 mm radius sphere with volume of 14.8 liters. The windows are made of quartz and have diameter of 190 mm and thickness of 50 mm. They are mounted parallel to each other, one in each hemisphere. The CVR is instrumented with K type thermocouples at the wall and at an internal position 75 mm from the center, static and dynamic pressure sensors, injection septum, spark plugs, and filling/emptying piping systems. The spark plugs have long prongs that form a 2 mm gap. The hemispheres and windows are sealed with o'ring seals. The heating system provides a maximum power of 1400 W. The maximum design temperature and pressure are 150 ^{o}C and 35 MPa, respectively.

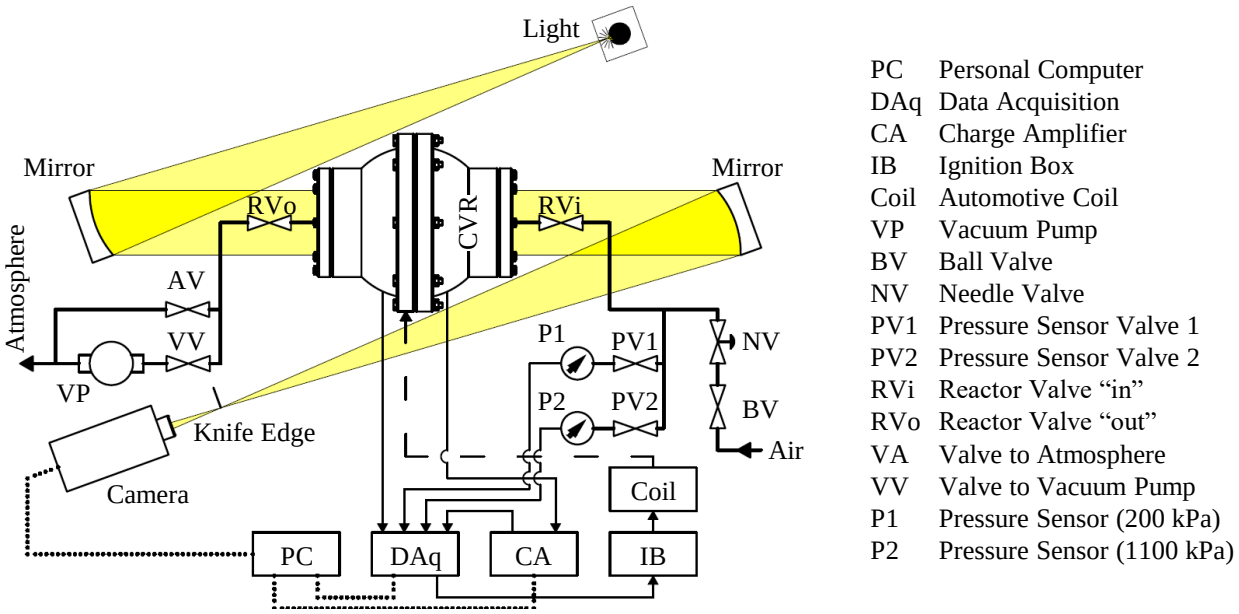

Figure 2. Rendering of the experimental apparatus. (Adapted from Monteiro (2015)).

The mass of liquid fuel m_f (g) in a given experiment is drawn in a precision syringe, measured in a scale and then injected in the reactor. The amount of air is controlled knowing the volume V_r (m^3), temperature T_u (K) and the static pressure p_u (Pa) measured in the reactor. Complete evaporation of the fuel and the ideal gas behavior are assumed (Monteiro, 2015).

Figure 3 presents typical radius and pressure versus time measured in the reactor for a mixture of iso-octane and air, at equivalence ratio $\phi = 1.002$, unburned pressure $p_u = 100.1$ kPa, unburned temperature $T_u = 398.3$ K. The mass of iso-octane injected in this condition is $m_f = 0.8479$ g. The measured laminar flame velocity is $S_L = 52.40$ cm/s and the burned Markenstein length is $L_b = 1.017$ mm (Monteiro, 2015).

Given the final measured values of laminar flame speed S_L obtained for a given fuel-air mixture, they are usually correlated to equivalence ratio ϕ, unburned pressure p_u, and unburned temperature T_u, using different semi-empiric equations. Metghalchi and Keck (1982) proposed a flame speed correlation function in the form

$$S_L = S_{L,ref} \left(\frac{T_u}{T_{ref}} \right)^{n_T} \left(\frac{p_u}{p_{ref}} \right)^{n_p} (1 - d_1 Y_{dil})^{d_2}, \tag{18}$$

where,

$$S_{L,ref} = a_0 + a_1\phi + a_2\phi^2 + a_3\phi^3, \quad n_T = b_0 + b_1\phi + b_2\phi^2, \quad n_p = c_0. \tag{19}$$

In this expression, Y_{dil} is the mass fraction of an inert in the reactant fuel-air mixture. The parameters for each mixture are a_0, a_1, a_2, a_3, b_0, b_1, b_2, c_0, d_1, d_2. When there is no diluent in the fuel-air mixture, $Y_{dil} = 0$. This expression presents a very good agreement to measurements in the entire flammability region. However, it is important not to exceed the flammability region or the equation may return unrealistic values. There is an extensive data-base of fuels curve-fitted to this equation and it will be used here.

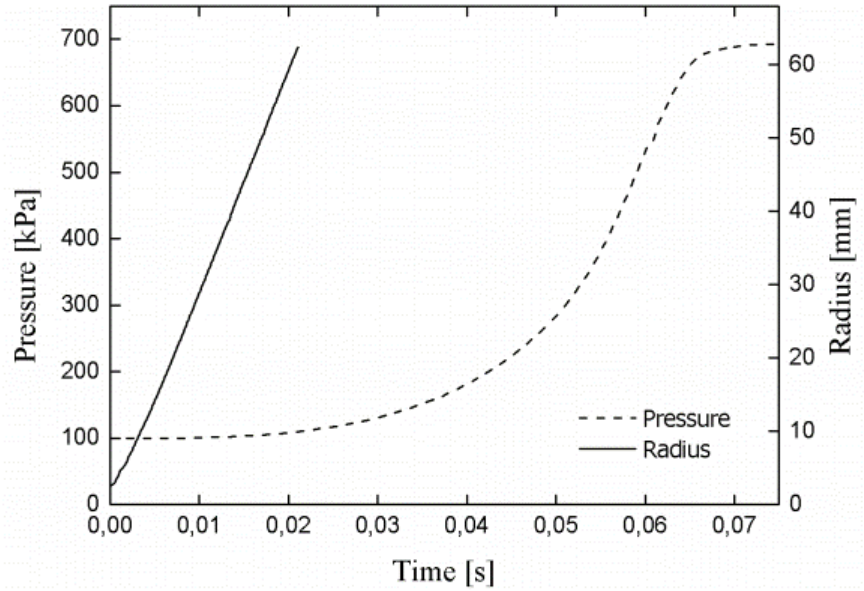

Figure 3. Flame radius R_F (mm) and pressure p (kPa) for a flame of iso-octane and air, at equivalence ratio $\phi = 1.002$, unburned pressure $p_u = 100.1$ kPa, and unburned temperature $T_u = 398.3$ K. The measured laminar flame velocity is $S_L = 52.40$ cm/s and the burned Markenstein length is $L_b = 1.017$ mm. (Monteiro, 2015).

3. ERROR PROPAGATION

It is assumed that y_j, $j = 1, 2, ..., M$, is a measurement output that depends on N input variables x_i, $i = 1, 2, ..., N$, thus, $y_j = f(x_1, x_2, ..., x_N)$. Here, the output variable is the laminar flame speed S_L and the input variables are the mass of fuel m_f, the unburned temperature T_u and pressure p_u. This dependence is expressed as $S_L = f(m_f, T_u, p_u)$

The input variables are set by an experimental matrix that defines the desired initial conditions for each test x_i. Their real values $x_{i,r}$, attained in a given run, are influenced by uncertainties in the set-up of the test, random errors in the measurement instruments used, and inaccuracies induced by the environment and the operator. Therefore, it is assumed that the measured values are accompanied by random errors and their expected values can be represented by

$$x_i = x_{i,d} \pm u_i. \tag{20}$$

In the Monte Carlo method, the random errors in the input variables u_i are assumed to follow a known probability distribution density $f(u_i)$. The method then reproduces the outcomes of a large number of runs, each of these runs affected by random errors. Assuming that the expected values of the random errors in the input variables x_i are $\bar{u}_i$ and making ξ a random variable with value $-\infty < \xi < \infty$ that follows a known probability distribution density, the error in the input variable is estimated as

$$u_i = \xi \bar{u}_i. \tag{21}$$

Table 1 summarizes the inputs for the calculation of laminar flame speed. The fuel is represented by a general chemical formula $C_\alpha H_\beta O_\gamma$. For a fuel made of a mixture of chemical species, the constants α, β and γ are such that the measured H/C ratio, H/O ratio, and molar mass are reproduced. The desired operating conditions for the measurement are the equivalence ratio, ϕ_d, the unburned temperature, $T_{u,d}$, and pressure, $p_{u,d}$.

Table 1. Inputs for the error propagation analysis for a fuel with general chemical formula $C_\alpha H_\beta O_\gamma$.

Desired operation conditions:

Equivalence ratio	nond.	ϕ_d
Initial temperature	K	$T_{u,d}$
Initial pressure	kPa	$p_{u,d}$
Hydrogen/carbon ratio	nond.	H/C = β/α
Oxygen/carbon ratio	nond.	O/C = γ/α

From the fuel composition and the desired values of T_u and p_u and ϕ, assuming simplified standard-dry air and ideal

air behavior (Law, 2010), the desired fuel mass $m_{f,d}$ is obtained from

$$m_{f,d} = \frac{\phi_d f_s M_a M_f}{M_f + \phi_d f_s M_a} \left(\frac{p_{u,d} V_r}{R_u T_{u,d}} \right), \quad f_s = \frac{M_f}{a_s M_a}, \quad a_s = \frac{2 \times \alpha + 0.5 \times \beta - \gamma}{0.21 \times 2}. \tag{22}$$

In the equations above, M_f and M_a (kg/kmol) are the molar masses of fuel and air, R_u (J/kmol-K) is the universal gas constant, $V_r = 14.3 \times 10^{-3}$ (m^3) is the volume of the reactor, f_s is the stoichiometric fuel/air mass ratio and a_s is the stoichiometry number of mols of air per mol of fuel.

Each of the input variables is accompanied by a random error. The best estimates of the input variables, following Eq. 21, are

$$m_f = m_{f,d} \pm u_m = m_{f,d} \pm \xi \, \bar{u}_m, \quad p_u = p_{u,d} \pm u_p = p_{u,d} \pm \xi \, \bar{u}_T, \quad T_u = T_{u,d} \pm u_T = T_{u,d} \pm \xi \, \bar{u}_p. \tag{23}$$

Form these best estimates, the mass of air m_a becomes

$$m_a = \frac{m_f}{f_s}. \tag{24}$$

The stoichiometric ratio becomes

$$\phi = \frac{M_f}{f_s M_a} \left(\frac{M_f V_r p_u}{R_u T_u m_f} - 1 \right)^{-1}. \tag{25}$$

The estimated laminar flame speed is then calculated using Eqs. (18) and (19). Finally, the effects of the errors in the input variables may be expressed as sensitivities.

Finally, a relative sensitivity of the relative error $u_{y,i}/y_i$ in the output variable y_i in respect to the relative error $u_{x,i}/x_i$ in the input variable x_i is calculated from

$$s_{y/x_i} = \frac{u_{y,i}/y_i}{u_{x,i}/x_i} = \frac{x_i}{y_i} \frac{u_{y,i}}{u_{x,i}}. \tag{26}$$

4. RESULTS AND ANALYSIS

A mixture of iso-octane ($\alpha = 8$, $\beta = 18$ and $\gamma = 0$) and air was selected for this study since it is representative of the behavior of oil derived, light, liquid fuels. Its flammability limits and flame speeds are typical of automotive fuels. The coefficients for the laminar flame speed correlation were obtained from (Monteiro, 2015) and are given in 2. Measurements for mixtures of iso-octane and air at $T_u = 398$ K and $p_u = 100$ kPa resulted in an average flame speed of 56,1 cm/s and confidence interval (for 95 % confidence level) of $\pm$ 1,2 cm/s, which is consistent with the values reported in the literature. Individual errors in mass, temperature, pressure and volume were estimated and are consistent with this overall error in flame speed. Table 3 presents an assessment of the measurement errors in mass, temperature, pressure and volume for the experiments in the CVR. Convergence of the Monte Carlo method was assumed after 10000 samples.

Table 2. Coefficients for the laminar flame speed correlation, lower flammability limit (LFL) and higher flammability limit (HFL). S_L is calculated in cm/s. The reference values are $T_{ref} = 398$ K, $p_{ref} = 100$ kPa (Monteiro, 2015).

Fuel	a_0	a_1	a_2	a_3	b_0	b_1	b_2	c_0	LFL	HFL
iso-octane	-88.73	211.26	-27.06	-42.59	5.11	-7.07	3.51	-0.2	0.469	1.626

Table 3. Typical values of confidence intervals (95 % coverage) for the input variables in experiments in the CVR.

Input variable	Estimated random error
Mass (mg)	$\pm$4.4
Temperature (K)	$\pm$2
Pressure (Pa)	$\pm$700
Volume (cm$_3$)	$\pm$10

Figure 4(a) presents the spread of the values of laminar flame speed calculated from the Monte Carlo runs considering the simultaneous effect of the typical errors on all input variables, at $T_u = 398$ K and $p_u = 100$ kPa. The results indicate that the effect of measurement errors increase towards the leaner and richer equivalence ratios, reaching a confidence interval (2 σ) of $\pm$ 3.5 % at $phi = 0.7$ and $\pm$ 3.6 % at $\phi = 1.4$. There is a minimum error bar of $\pm$ 0.72 % at $\phi = 1.16$. The behavior illustrated in this figure can be better explored as the effects of each individual variables are sorted out.

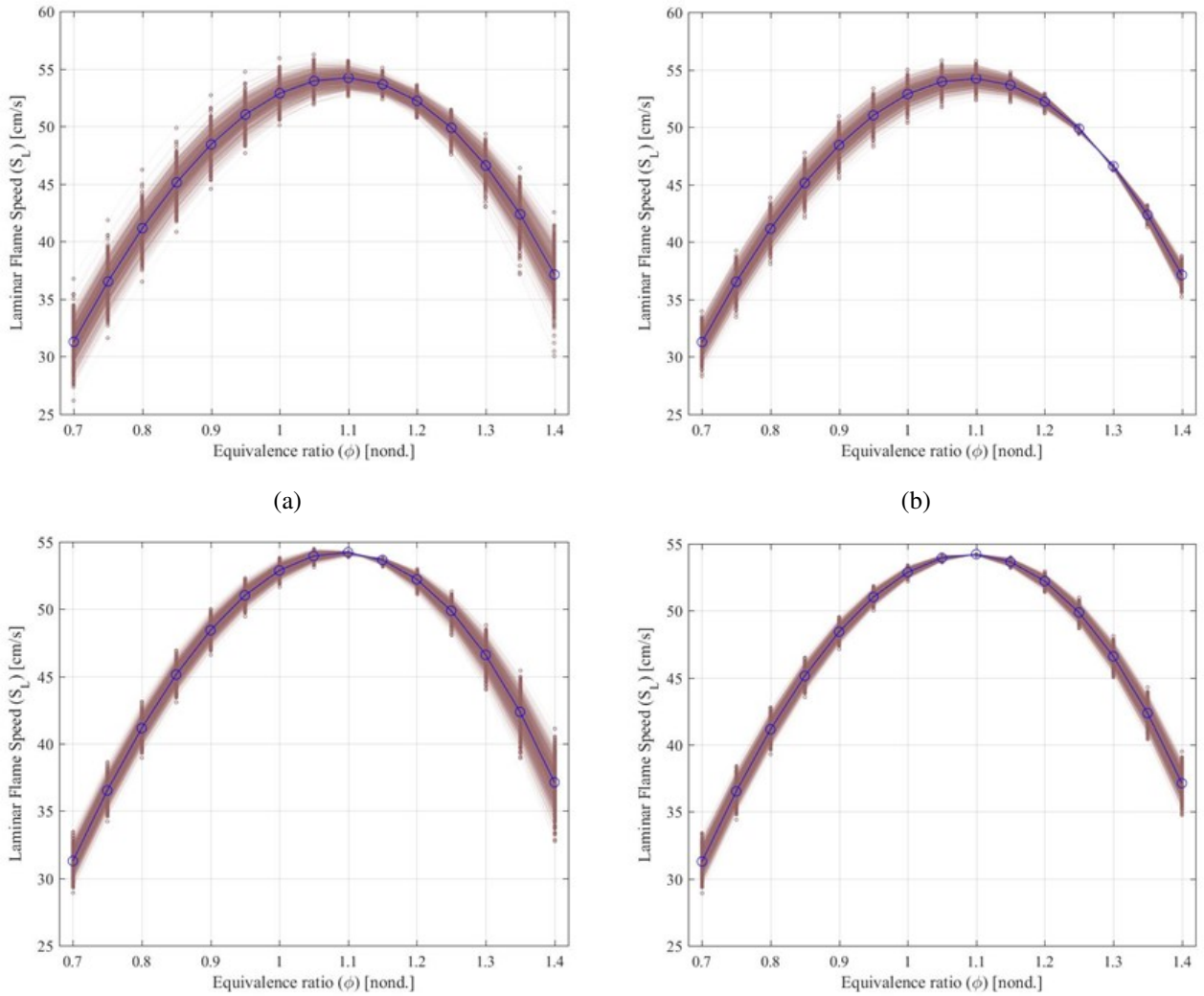

Figure 4. Values of laminar flame speed S_L as a function of equivalence ratio ϕ calculated from the Monte Carlo runs considering (a) the simultaneous effect of the typical errors on all input variables and the individual effects of the errors in (b) T_u, (c) p_u and (d) m_f at $T_u = 398$ K and $p_u = 100$ kPa. See Table 3 for the magnitude of the individual errors.

Figure 4(b) presents the values of laminar flame speed calculated from the Monte Carlo runs considering the individual effects of the errors in T_u, at $T_u = 398$ K and $p_u = 100$ kPa. The errors in S_L caused by errors in T_u have a minimum at $\phi = 1.27$, as a result of the combined effects of T_u in ϕ and directly in S_L. Figures 4(c) and (d) present the effects of the errors in p_u and m_f. Both errors have no effect on S_L at $phi = 1.1$, where S_L reaches a maximum ($dS_L/d\phi = 0$). This means that the effect of the errors in p_u directly in S_L are small, and the errors in p_u and m_f mostly affect S_L through ϕ. The behavior displayed in Figure 4(a) is a combination of these three effects.

Figure 5(a) summarizes the confidence intervals illustrated in Figure 4(b). At $\phi = 0.7$, all errors contribute approximately equally to the the total error in S_L. At $\phi = 1$, the error in S_L is entirely due to the errors in T_u. Conversely, at $\phi = 1.4$, the errors in S_L are primarily due to the errors in p_u and m_f. The confidence interval in the values of S_L for $0.4 \leq \phi \leq 1.4$ remains under $\pm$ 3.5 %.

Figure 5(b) presents the relative sensitivities of the individual errors in the errors in laminar flame speed, according to Eq. 26. The relative sensitivities are calculated assigning random relative errors of 1 % of the desired value to each variable. The relative sensitivity expresses the relative importance of the errors in T_u at low ϕ and of p_u and m_f at higher ϕ. Figure 5(b) also indicates that, at low ϕ, positive errors in T_u and m_f result in positive errors in S_L while the opposite occurs with the errors in p_u and V_r. This situation is inverted at high ϕ. The sensitivities presented in figure 5(b) are listed in Table 4. At higher temperatures, the effect of temperature in the overall errors is reduced. The relative errors are insensitive to the increase in pressure. We note that the errors in ϕ have a practically direct sensitivity to the errors in the input variable. In this table, the sensitivities of the errors in H/C ratio are also included. However, these sensitivities were calculated considering only their effect in ϕ, not the direct effect on S_L, since these would require a more complete model

of laminar flame speed.

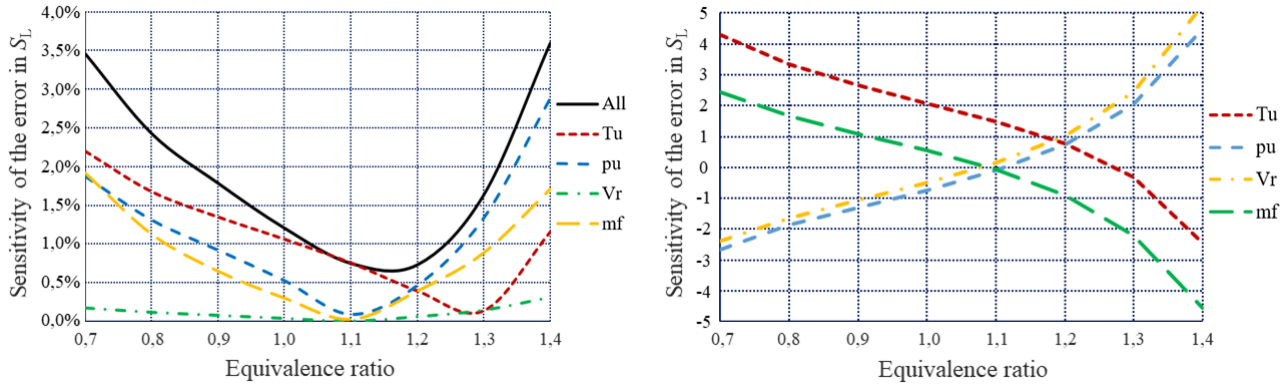

Figure 5. (a) Confidence intervals (2 σ) in the laminar flame speed S_L as a function of equivalence ratio assuming isolated errors in each input variable (T_u, p_u, m_f, H/C) and the simultaneous effect of the errors in all input variables (all), and (b) relative sensitivities of the individual errors in the errors in laminar flame speed (according to Eq. 26). Calculations for iso-octane/air, at $T_u = 398$ K and $p_u = 100$ kPa.

Table 4. Sensitivity of the errors in S_L and ϕ in respect to the errors in the input variables, calculated for 1 % error in the input variables. The first three columns are the desired conditions, the next 5 are the sensitivities of the error in S_L to the error in each input variable individually (the remaining are set to zero), the next column is the overall error in S_L when all variables present 1 % error simultaneously, and the remaining 6 columns are the same estimates for ϕ. The fuel is iso-octane, with H/C = 2.25.

Condition			S_L						ϕ					
ϕ	T_u	p_u	T_u	p_u	V_r	m_f	H/C	all	T_u	p_u	V_r	m_f	H/C	all
nond.	K	kPa	nond.	nond.	nond.	nond.	nond.	nond.	nond.	nond.	nond.	nond.		
0.7	398	100	4.40	2.66	2.47	2.51	0.61	6.20	1.02	1.00	1.00	1.02	0.21	2.02
1.1	398	100	1.51	0.13	0.06	0.06	0.06	1.47	1.02	1.01	1.02	1.02	0.21	2.04
1.4	398	100	2.28	4.14	4.26	4.41	1.21	7.79	1.02	1.04	1.02	1.02	0.22	2.01
0.7	498	100	4.04	2.37	2.18	2.16	0.45	5.58	1.02	1.02	1.02	1.01	0.21	2.03
1.1	498	100	1.67	0.30	0.10	0.10	0.02	1.70	1.01	1.02	1.01	1.02	0.22	2.04
1.4	498	100	1.42	3.29	3.50	3.52	0.75	6.07	1.02	1.01	1.04	1.03	0.22	2.06
0.7	398	500	4.41	2.65	2.50	2.48	0.52	6.15	1.02	0.99	1.01	1.01	0.21	2.00
1.1	398	500	1.49	0.13	0.06	0.06	0.01	1.50	1.00	1.00	1.01	0.99	0.22	2.04
1.4	398	500	2.30	4.14	4.43	4.36	0.95	7.90	1.02	1.01	1.03	1.03	0.22	2.07

5. CONCLUSION

Here, the error propagation in the measurement of laminar flame speed from the outwardly propagation of spherical flames in constant volume reactors is estimated using a Monte Carlo method.

The base case for analysis considered a mixture of iso-octane and air at $T_u = 398$ K and $p_u = 100$ kPa with typical errors (90 % confidence intervals) of ± 2 K in T_u, ± 700 Pa in p_u, ± 4.4 mg in m_f and ± 10 cm^3 in V_r. Under these conditions, typical of measurements in CVR, the results indicated that the effect of measurement errors in the input variables increase towards the leaner and richer equivalence ratios, reaching a confidence interval (2 σ) of $\pm$ 3.5 % at $phi = 0.7$ and $\pm$ 3.6 % at $\phi = 1.4$. There is a minimum error bar of $\pm$ 0.72 % at $\phi = 1.16$. The confidence interval in the values of S_L for $0.4 \leq \phi \leq 1.4$ remains under $\pm$ 3.5 %.

Considering the individual effects of each input variable in the laminar flame speed, it was observed that the errors in S_L caused by errors in T_u have a minimum at $\phi = 1.27$, as a result of the combined effects of T_u in ϕ and directly in S_L. The errors in p_u and m_f have no effect on S_L at $phi = 1.1$, where S_L reaches a maximum ($dS_L/d\phi = 0$). This means that the effect of the errors in p_u directly in S_L are small, and the errors in p_u and m_f mostly affect S_L through ϕ.

The analysis of relative sensitivity showed that the errors in T_u are more important at low ϕ and those of p_u and m_f at higher ϕ. Also, at low ϕ, positive errors in T_u and m_f result in positive errors in S_L while the opposite occurs with the errors in p_u and V_r. This situation is inverted at high ϕ. The errors in ϕ have a practically direct sensitivity to the errors

in the input variable. At higher temperatures, the effect of temperature in the overall errors is reduced. The relative errors are insensitive to the increase in pressure.

The results indicate that a relatively very precise measurement can be obtained at ϕ around stoichiometry by just minimizing the errors in T_u, since the errors in the remaining input variables have relatively small importance at this equivalence ratio. The minimization of errors in T_u require a uniform heating of the reactor and the measurement of temperature in several positions around the reactor, assigning the average black-body cavity temperature, i.e., the average T^4 temperature, as average T_u. Also, higher T_u contribute to the reduction of the effects of the errors in temperature.

6. REFERENCES

Bauwens, C.R.L., Bergthorson, J.M. and Dorofeev, S.B., 2019. "Modeling the formation and growth of instabilities during spherical flame propagation". *Proceedings of the Combustion Institute*, Vol. 37, No. 3, pp. 3669 – 3676.

Beeckmann, J., Hesse, R., Schaback, J., Pitsch, H., Varea, E. and Chaumeix, N., 2019. "Flame propagation speed and markstein length of spherically expanding flames: Assessment of extrapolation and measurement techniques". *Proceedings of the Combustion Institute*, Vol. 37, No. 2, pp. 1521 – 1528.

Bonhomme, A., Selle, L. and Poinsot, T., 2013. "Curvature and confinement effects for flame speed measurements in laminar spherical and cylindrical flames". *Combustion and Flame*, Vol. 160, No. 7, pp. 1208 – 1214.

Bradley, D., Lawes, M. and Morsy, M., 2019. "Flame speed and particle image velocimetry measurements of laminar burning velocities and markstein numbers of some hydrocarbons". *Fuel*, Vol. 243, pp. 423 – 432.

Chen, Z., 2011. "On the extraction of laminar flame speed and markstein length from outwardly propagating spherical flames". *Combustion and Flame*, Vol. 158, No. 2, pp. 291 – 300.

Chen, Z., 2015. "On the accuracy of laminar flame speeds measured from outwardly propagating spherical flames: Methane/air at normal temperature and pressure". *Combustion and Flame*, Vol. 162, No. 6, pp. 2442 – 2453.

Egolfopoulos, F.N., 2012. "Laminar flame speed: What do we measure? what do we report? what do we learn? how do we use it?" In *Workshop "New Perspectives for Laminar Burning Velocity", CORIA Laboratory, Rouen, France*.

Faghih, M., Li, H., Gou, X. and Chen, Z., 2019. "On laminar premixed flame propagating into autoigniting mixtures under engine-relevant conditions". *Proceedings of the Combustion Institute*, Vol. 37, No. 4, pp. 4673 – 4680.

Giannakopoulos, G.K., Frouzakis, C.E., Mohan, S., Tomboulides, A.G. and Matalon, M., 2019. "Consumption and displacement speeds of stretched premixed flames - theory and simulations". *Combustion and Flame*, Vol. 208, pp. 164 – 181.

Hartmann, E.M., 2014. *Instrumentation and operacionalization of a constant volume reactor to measure laminar flame speed (in Portuguese)*. Master's thesis, Federal University of Santa Catarina, Florianópolis, Brasil.

Herrador, A.M. and Gonález, A.G., 2004. "Evaluation of measurement uncertainty in analytical assays by means of monte-carlo simulation". *Talanta*, Vol. 64, No. 2, pp. 415–422.

Huo, J., Yang, S., Ren, Z., Zhu, D. and Law, C.K., 2018. "Uncertainty reduction in laminar flame speed extrapolation for expanding spherical flames". *Combustion and Flame*, Vol. 189, pp. 155 – 162.

Jayachandran, J., Lefebvre, A., Zhao, R., Halter, F., Varea, E., Renou, B. and Egolfopoulos, F.N., 2015. "A study of propagation of spherically expanding and counterflow laminar flames using direct measurements and numerical simulations". *Proceedings of the Combustion Institute*, Vol. 35, No. 1, pp. 695 – 702.

Jayachandran, J., Zhao, R. and Egolfopoulos, F.N., 2014. "Determination of laminar flame speeds using stagnation and spherically expanding flames: Molecular transport and radiation effects". *Combustion and Flame*, Vol. 161, No. 9, pp. 2305 – 2316.

Kelley, A. and Law, C., 2009. "Nonlinear effects in the extraction of laminar flame speeds from expanding spherical flames". *Combustion and Flame*, Vol. 156, No. 9, pp. 1844 – 1851.

Law, C.K., 2010. *Combustion Physics*. Cambridge University Press, 1st edition.

Lefebvre, A., Larabi, H., Moureau, V., Lartigue, G., Varea, E., Modica, V. and Renou, B., 2016. "Formalism for spatially averaged consumption speed considering spherically expanding flame configuration". *Combustion and Flame*, Vol. 173, pp. 235 – 244.

Liang, W., Wu, F. and Law, C.K., 2017. "Extrapolation of laminar flame speeds from stretched flames: Role of finite flame thickness". *Proceedings of the Combustion Institute*, Vol. 36, No. 1, pp. 1137 – 1143.

Lipatnikov, A.N., Shy, S.S. and yi Li, W., 2015. "Experimental assessment of various methods of determination of laminar flame speed in experiments with expanding spherical flames with positive markstein lengths". *Combustion and Flame*, Vol. 162, No. 7, pp. 2840 – 2854.

Metghalchi, M. and Keck, J.C., 1982. "Burning velocities of mixtures of air with methanol, isooctane, and indolene at high pressure and temperature". *Combustion and Flame*, Vol. 48, pp. 191 – 210.

Moghaddas, A., Eisazadeh-Far, K. and Metghalchi, H., 2012. "Laminar burning speed measurement of premixed n-decane/air mixtures using spherically expanding flames at high temperatures and pressures". *Combustion and Flame*, Vol. 159, No. 4, pp. 1437 – 1443.

Monteiro, J.O.D., 2015. *Laminar flame speed of fuel mixtures applied to spark ignition internal combustion engines*. Master's thesis, Federal University of Santa Catarina, Florianópolis, Brasil.

Omari, A. and Tartakovsky, L., 2016. "Measurement of the laminar burning velocity using the confined and unconfined spherical flame methods – a comparative analysis". *Combustion and Flame*, Vol. 168, pp. 127 – 137.

Park, O., Veloo, P.S., Sheen, D.A., Tao, Y., Egolfopoulos, F.N. and Wang, H., 2016. "Chemical kinetic model uncertainty minimization through laminar flame speed measurements". *Combustion and Flame*, Vol. 172, pp. 136 – 152.

Wu, F., Liang, W., Chen, Z., Ju, Y. and Law, C.K., 2015. "Uncertainty in stretch extrapolation of laminar flame speed from expanding spherical flames". *Proceedings of the Combustion Institute*, Vol. 35, No. 1, pp. 663 – 670.

Xiouris, C., Ye, T., Jayachandran, J. and Egolfopoulos, F.N., 2016. "Laminar flame speeds under engine-relevant conditions: Uncertainty quantification and minimization in spherically expanding flame experiments". *Combustion and Flame*, Vol. 163, pp. 270 – 283.

Yu, H., Han, W., Santner, J., Gou, X., Sohn, C.H., Ju, Y. and Chen, Z., 2014. "Radiation-induced uncertainty in laminar flame speed measured from propagating spherical flames". *Combustion and Flame*, Vol. 161, No. 11, pp. 2815 – 2824.

7. RESPONSIBILITY NOTICE

The authors are the only responsible for the printed material included in this paper.